## PAPER

Check for updates

# Heat and pressure-resistant room temperature irreversible sealing of hybrid PDMS–thermoplastic microfluidic devices *via* carbon–nitrogen covalent bonding and its application in a continuous-flow polymerase chain reaction†

Rajamanickam Sivakumar, [ID] [a] Kieu The Loan Trinh [ID] [a] and Nae Yoon Lee [ID] *[b]

In this study, we have introduced a facile room-temperature strategy for irreversibly sealing polydimethylsiloxane (PDMS) elastomers to various thermoplastics using (3-aminopropyl)triethoxysilane (APTES) and [2-(3,4-epoxycyclohexyl)ethyl]trimethoxysilane (ECTMS), which can resist heat and pressure after sealing due to the high chemical reactivity of the used chemicals. An irreversible chemical bond was realized at RT within 30 min through the initial activation of PDMS and thermoplastics using oxygen plasma, followed by surface modification using amino- and epoxy-based silane coupling reagents on either side of the substrates and then conformally contacting each other. Surface characterizations were performed using contact angle measurements, fluorescence measurements, X-ray photoelectron spectroscopy (XPS), and atomic force microscopy (AFM) to verify the successful surface modification of PDMS and thermoplastics. The tensile strengths of the bonded devices were 274.5 ± 27 (PDMS–PMMA), 591.7 ± 44 (PDMS–PS), 594.7 ± 25 (PDMS–PC), and 510 ± 47 kPa (PDMS–PET), suggesting the high stability of interfacial bonding. In addition, the results of the leakage test revealed that there was no leakage in the indigenously fabricated hybrid devices, even at high pressures, which is indicative of the robust bond strength between PDMS and thermoplastics obtained through the use of the chemical bonding method. Moreover, for the first time, the heat and pressure-resistant nature of the bonded PDMS–PC microfluidic device was assessed by performing a continuous-flow polymerase chain reaction (CF-PCR), which requires a high temperature and typically generates a high pressure inside the microchannel. The results demonstrated that the microfluidic device endured high heat and pressure during CF-PCR and successfully amplified the 210 bp gene fragment from the Shiga-toxin gene region of *Escherichia coli* (*E. coli*) O157:H7 within 30 min.

## Introduction

A well-established technology is necessary for integrating complex microfluidic components, such as micro-pumps, micro-valves, and reservoirs, for the fabrication of a functional Lab-on-a-Chip (LOC) or microfluidic bioassay. To this end, the Micro Total Analysis System (μTAS) has been developed; however, the limitations of μTAS are that it is accessible only for silicon and related substrates and involves high fabrication cost due to the use of silicon. Hence, polymers were introduced to

develop hybrid functional devices, but they were initially necessary only in the fabrication of a few parts of LOCs.[1] However, in recent years, polymer micro-technology has become more versatile and reliable to facilitate the design and construction of all polymeric LOCs.

PDMS is one of the preferred materials in hybrid micro-fluidic device fabrication and has many advantages over silicon and glass, such as flexibility, affordable price, and optical transparency. Additionally, PDMS can be modified into complex shapes within a short time and unlike silicon and glass, PDMS does not require an expensive cleanroom facility. Furthermore, PDMS can easily bond to other PDMS or silicon-like substrates by a simple surface activation method, and this property can be useful for the fabrication of disposable low-cost LOCs.[2] Thermoplastics are also materials for hybrid frameworks, and these substrates have many attractive properties, such as high optical transparency, low thermal conductance, and good biocompatibility, which make them promising materials for bio-

*[a] Department of Industrial Environmental Engineering, College of Industrial Environmental Engineering, Gachon University, 1342 Seongnam-daero, Sujeong-gu, Seongnam-si, Gyeonggi-do, 13120, Korea*

*[b] Department of BioNano Technology, Gachon University, 1342 Seongnam-daero, Sujeong-gu, Seongnam-si, Gyeonggi-do, 13120, Korea. E-mail: nylee@gachon.ac.kr*

† Electronic supplementary information (ESI) available. See DOI: 10.1039/d0ra02332a

microelectromechanical system (bio-MEMS) calorimeters,[3] electrochemical LOC,[4] and other biosensor applications.[5] Despite the many advantages of PDMS and thermoplastics, the strong sealing between the two substrates is one of the important aspects of the fabrication of LOCs. The strong sealing of the devices makes it possible to inject the fluids at high pressure, perform the experiments at high temperature, and avoid external contamination during device function.

To produce high-sealing devices, several bonding techniques have been developed. Overall, these techniques can be divided into two categories: (1) direct bonding and (2) indirect bonding. The former method, which includes thermal bonding, solvent bonding, and adhesive bonding, *etc.*, requires high temperature and pressure to obtain mostly plastic–plastic devices and each method has its advantages and limitations. For instance, some bonding methods could change the channel dimensions by clogging, or alter the channel wall properties due to the high temperature and pressure. Moreover, the latter method (indirect bonding) has used several techniques to circumvent the channel clogging by using an intermediate substance to seal the two incompatible surfaces. The intermediate substances, such as glycidyl methacrylate,[6,7] and 3-(trimethoxysilyl)propyl methacrylate[8] have been cured by UV light or elevated temperature, which act as an adhesive for the bonding of PDMS with non-silicon-based materials. More significantly, the chemicals (3-aminopropyl)triethoxysilane (APTES) and (3-glycidyloxypropyl) trimethoxysilane (GPTMS) have been commonly used in many approaches for bonding PDMS to polyethylene terephthalate,[9] polycarbonate,[10–12] cyclic olefin copolymer,[13] and poly(methyl methacrylate).[14] Other chemicals, including 3-mercaptopropyl-trimethoxysilane (MPTMS),[15] bis[3-(triethoxysilyl)propyl]amine (BTESPA),[16] and bis[3-(trimethoxysilyl)propyl]amine (BTMSPA),[17] have also been introduced to bond thermoplastic or porous membranes to PDMS. However, most of the reported methods mentioned above have some limitations, such as longer times for the fabrication process and the requirement of high temperature and pressure for bond formation. In contrast, in the present study, we have fabricated high-strength hybrid microfluidic devices at RT with less fabrication time; these devices do not require additional pressure for bonding, which may be attributed to the usage of the highly reactive ring-strained cyclohexyl epoxysilane (ECTMS) that induces stronger bond formation between the PDMS and thermoplastics.

Recently, in the microfluidic chips for testing *trans*-epithelial electrical resistance (TEER) and anti-cancer drugs, 3-APTES and GPTMS have been used as silane reagents in device fabrication.[11,12,18] The results of evaluating these microfluidic devices revealed that the silane reagents are compatible with cells without inhibiting cell growth in the microfluidic channels. Based on these findings, in the present study, we presume that ECTMS containing microfluidic devices can be used to perform various applications, such as polymerase chain reactions, cell culture experiments, and evaporation-based protein crystallization, since both the chemical and physical properties of ECTMS and GPTMS are almost analogous.

In recent years, the process of polymerase chain reaction (PCR) has been widely used to replicate DNA and, particularly, to produce copies of specific fragments of DNA by thermal cycling through three different temperatures. The quantity of DNA can be multiplied in each temperature cycle, which subsequently generates millions of DNA copies between 20 and 35 cycles. Nowadays, the development of miniaturized PCR devices has gained more attention;[19–21] in the design of miniaturized PCR devices, continuous-flow-high-throughput PCR (CF-PCR) has many advantages. For instance, the temperature controlling system is much easier than chamber-based PCR, and the PCR mixture is pumped into a straight,[22] serpentine,[23,24] or circular[25,26] microfluidic channel through the continuous flow with fixed temperature zones. The results obtained through the PCR process are highly accurate and reliable; therefore, it has been widely used in various fields including food sciences,[27] agricultural sciences,[28] and biomedical applications.[29] Apart from PCR, the chemical and biological reactions were simultaneously monitored effectively with different concentrations of reagent using the microfluidics devices.[30]

The present study aims to design stable and economic hybrid microfluidic devices that can tolerate high temperature and pressure using robust bonding strategies between PDMS and thermoplastic materials. This technique is based on the surface modification of the materials to be bonded. Briefly, both polymeric substrates are initially plasma-activated and then the terminal epoxy groups are introduced on the surface of the PDMS using 1% aqueous ECTMS, whereas terminal amine groups are introduced on the surface of the thermoplastics using 1% aqueous APTES. Finally, irreversible bonding occurs when the coated substrates contact each other at RT for 30 min as a result of the strong carbon–nitrogen (C–N) covalent bond formation between the two surfaces. Furthermore, the high pressure and thermal stability of the fabricated hybrid PDMS–PC microfluidic device was used to perform the CF-PCR to amplify a 210 bp gene fragment from the Shiga-toxin gene region of *Escherichia coli* (*E. coli*) O157:H7. To the best of our knowledge, there have been no previous reports on chemically surface-coated substrates to fabricate hybrid PDMS–PC microfluidic devices for CF-PCR applications that require such high bonding strength and temperature to amplify the DNA for foodborne pathogen detection.

## Materials and methods

### Chemicals and materials

(3-Aminopropyl)triethoxysilane (APTES; 99%) and [2-(3,4-epoxycyclohexyl)ethyl]trimethoxysilane (ECTMS; 98%) were purchased from Sigma-Aldrich. The PDMS prepolymer (Sylgard 184) and curing agent were obtained from Dow Corning. Poly(methyl methacrylate) (PMMA), polycarbonate (PC), polystyrene (PS), and polyethylene terephthalate (PET) were purchased from Goodfellow. Fluospheres amine (0.2 μm, red) and TE buffer (10 nM Tris–HCl, 0.1 nM EDTA, pH 8.0) were obtained from Thermo Fisher Scientific. *Taq* polymerase, PCR buffer solutions, and dNTPs were obtained from BioFact (Daejeon, Korea). Agarose powder was purchased from BioShop (Ontario, Canada). A 100 bp DNA size marker was purchased from Takara (Shiga, Japan). Ethidium bromide (EtBr)-based dye (Loading STAR) was purchased from Dynebio (Seongnam, Korea).

## Chemical bonding of PDMS to thermoplastics

The surface of the PDMS and thermoplastics were separately coated by using different chemicals such as ECTMS and APTES. The schematic process flow for bonding PDMS with thermoplastics is shown in Fig. 1. In this experiment, a flat elastomeric PDMS sheet was produced after the thermal curing of PDMS prepolymer and curing agent (10 : 1 ratio) at 80 °C for 2 h. Before plasma treatment, the PDMS sheet and thermoplastics were washed with methanol, rinsed with deionized water, and then air-dried. Then, the PDMS sheet and thermoplastics were oxidized by oxygen plasma treatment for 1 min, which was followed by treatment with aqueous ECTMS (1 wt%) for PDMS and aqueous APTES (1 wt%) for thermoplastics at RT for 30 min. Next, both substrates were washed with water, methanol, dried with air, and immediately bonded with each other to form an irreversible bond *via* carbon–nitrogen covalent bonding. The time-lapse progress of the reaction is displayed as Fig. S1 in the ESI.† For better results, the 1 wt% ECTMS solution was stirred at RT for 90 min at the beginning, then plasma-activated PDMS was immersed in it. Generally, ECTMS is used as a coupling agent or adhesion promoter because terminal cyclic epoxide groups are highly reactive electrophiles that can react with common nucleophiles such as –NH$_2$, –SH, and –OH. Hence, we made ECTMS-coated PDMS as an adhesive to covalently link with APTES-coated thermoplastics realized by the carbon–nitrogen bond (C–N bond) formation.

## Surface characterizations

The contact angle measurements (Phoenix 300, Surface Electro-Optics, South Korea), fluorescence measurements (ProgRes CapturePro software), X-ray photoelectron spectroscopy, and atomic force microscopy (JPK NanoWizard II) were performed to characterize the functionalized surface. The XPS analyses were performed using an AxisHsi (Kratos Analytical, UK) equipped with an aluminum X-ray source (mono-gun, 1486.6 eV) with the pass energy of 40 eV. The pressure in the chamber was below $5 \times 10^{-9}$ Torr before the data were recorded, and the voltage and current of the anode were 13 kV and 18 mA, respectively. The take-off angle was set at 45°. The binding energy of C1s (284.5 eV) was used as the reference. The resolution for the measurement of the binding energy was about 0.1 eV.

## Analysis of the bonding strength

**Tensile test.** We evaluated the bonding strength between the PDMS and thermoplastics using a texture analyzer (QTS 25, Brookfield, Middleboro, MA, USA). In this experiment, a thick twine was put into the PDMS prepolymer and was cured at 80 °C for 2 h. For another end, a single hole was made in thermoplastics using a high-speed drill machine (Woosung E&I Co, LTD, Korea), and the twine was inserted through the hole. After bonding, these two substrates were pulled at the speed of 100 mm min$^{-1}$, and the experiments were repeated in triplicate to confirm the reproducible bonding strength of the hybrid devices.

**Leakage test.** The thermoplastic containing a serpentine microchannel with a depth of 2 mm, a width of 2 mm, and a total length of 100 mm was bonded to a flat PDMS. Inlet and outlet holes were punched on the PDMS side in the positions corresponding to the two terminal ends of the microchannel engraved on the thermoplastics for fluid infusion. The silicone tubes (o.d. 2 mm and i.d. 1 mm) were directly inserted into the punched holes and then glued using a 10 : 1 (w/w) mixture of the PDMS prepolymer and a curing agent. For better visualization, the purple ink solution was injected into the microchannel and flow rates were systematically controlled at 0.1, 1.0, 10, 20, and 30 mL min$^{-1}$ using a syringe pump. In addition, the burst test was conducted for the hybrid microfluidic devices by introducing compressed air into the microchannel through the silicon inlet and monitoring the maximum pressure when the bonded devices were disassembled.
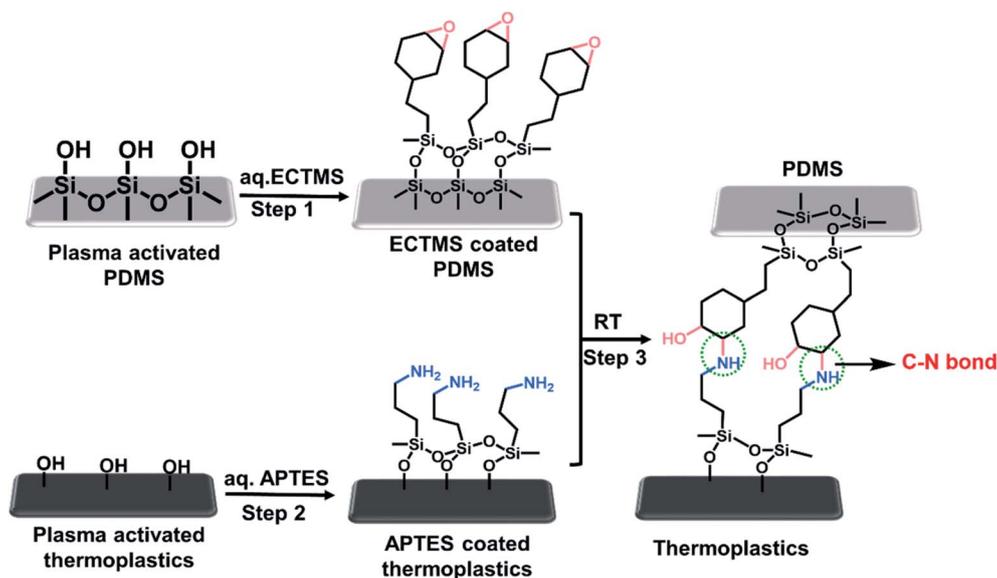


**Fig. 1** Scheme for the fabrication of PDMS–thermoplastic microfluidic devices.

**Hydrolytic stability test.** The microfluidic devices used in the hydrolytic study had a similar design and dimensions to those used in the leakage test. To examine the hydrolytic stability of the bonded interfaces, one of the fabricated microfluidic devices was immersed in water for 3 days at 40 °C, and another one at 90 °C for 12 h, followed by injecting water into the microchannels using a syringe pump.

### Temperature measurements for performing CF-PCR

The two-temperature measurement, including denaturation and annealing/extension, was applied for on-chip CF-PCR using a hybrid PDMS–PC microfluidic device. An infrared (IR) camera (FLIR Thermovision A320) was used to measure the surface temperature of the PC substrate. Also, the temperature controller was used for controlling the temperature during the PCR process as shown in Fig. S2 in the ESI.† In this procedure, the temperatures of two copper heaters were separately controlled for denaturation and annealing/extension as described in our previous studies.[31–34] The temperature measured on the surface of the copper heaters was considered to be the temperature inside the microchannel since the PC where the microchannel was engraved was only 2 mm in thickness, and the relatively low thermal conductivity of the PC $(0.22 \text{ W K}^{-1} \text{ m}^{-1})$ prevented heat dissipation and confined heat within the PC. The surface of the PC was then covered with black tape to reduce the heat reflection during temperature measurement using an IR camera. Ten spots were randomly selected for temperature measurement, and the average temperature was evaluated using an image analyzer (Therma-CAM researcher 2.8). The temperature for the annealing/extension zone was 56.91 ± 0.21 °C, and that for the denaturation zone was 94.63 ± 0.38 °C. Also, to ensure the stability of the device, the temperature was continuously observed over 2 h.

### Procedures for CF-PCR

For PCR application, a PDMS–PC microfluidic device (4.5 × 4.5 cm) with a serpentine microchannel with the width, depth, and total length of 300 μm, 200 μm, and 180 cm, respectively, was fabricated. The schematic illustration of the serpentine microchannel of a PDMS–PC microfluidic device is shown in Fig. S3 in the ESI.† For DNA templates used in the PCR processes, *E. coli* O157:H7 was collected from a liquid culture solution, and its DNA was directly isolated and added to the PCR reagents. The primer sequences for amplifying a 210 bp DNA fragment of the Shiga-toxin gene in *E. coli* O157:H7 were as follows: 5′-TGT AAC TGG AAA GGT GGA GTA TAC A-3′ (forward) and 5′-GCT ATT CTG AGT CAA CGA AAA ATA AC-3′ (reverse). The PCR mixture contained 5 μL buffer, 0.16 mM dNTPs mixture, 0.5 μM forward and reverse primers and 0.5 U μL$^{-1}$ of Taq polymerase. For the on-chip amplification, the inner surface of the microchannel was passivated with a BSA solution (1.5 mg mL$^{-1}$) to reduce the nonspecific adsorption of the PCR reagent on the walls of the microchannel. Next, the PCR reagent was introduced into the microchannel at 4 μL min$^{-1}$, and amplifications were performed for 30 thermal cycles. PCR results were analyzed by using the gel electrophoresis method and were observed by

*trans*-illuminated UV light using a Bio-Rad Molecular Imager Gel-Chem-Doc XR imaging system (Bio-Rad Laboratories, Hercules, CA, USA).

## Results and discussion

### Surface analysis

The oxygen plasma treatment is an excellent technique for increasing the hydrophilic properties of polymers since it can produce many hydroxyl groups (–OH) on the surface of the polymers, enabling the versatile chemical modification of the surface. Various analysis techniques, including contact angle measurements, fluorescence measurements, XPS measurements, and atomic force microscope (AFM) techniques, were performed to confirm the successful surface modification of PDMS and thermoplastics. The corresponding experimental results are discussed below.

**Contact angle measurement.** To confirm our bonding strategy between PDMS and thermoplastics, we first examined the surface functionalization of the substrates by measuring the contact angles. The contact angle of the hydrophobic PDMS was 110.5 ± 0.4° but it dramatically changed to a hydrophilic nature after the oxygen plasma treatment (contact angle < 10°). When the surface was further treated with ECTMS, the contact angle increased to 71.8 ± 3.6° due to the formation of the hydrophobic siloxane bond (Fig. 2a). Based on this initial observation, ECTMS was successfully attached to the surface of the PDMS.[35]

**Fluorescence measurement.** The amine-modified fluorescent microspheres (2 μm in diameter), with excitation and emission at 580 nm and 605 nm, respectively, were used to confirm the successful coating of ECTMS on the PDMS surface. The fluorescence microscopy images showing the pristine PDMS and ECTMS-coated PDMS after being treated with an amine-modified microsphere solution are shown in Fig. 2b. The ECTMS-coated PDMS displayed strong fluorescence as the amine (–NH₂) microsphere acted as a nucleophile and aggressively reacted with the active electrophile of the terminal epoxy group of the ECTMS coated on the PDMS, which created a strong covalent bond. On the other hand, the pristine PDMS did not show any fluorescence, suggesting that there was no chemical reaction on its surface.

**XPS analysis.** In order to examine the attachment of the chemicals on the surface of the PDMS and PC, X-ray photoelectron spectroscopy (XPS) was used to analyze the pristine and modified substrates. The XPS analysis results revealed that the silane reagent APTES reacted on the surface of the PC (Fig. 3a and d). General survey spectra of pristine PC, APTES-coated PC, and their individual spectra, such as carbon (C1s), oxygen (O1s), nitrogen (N1s), and silicon (Si2p), are shown in Fig. 3a–f. The survey spectrum of pristine PC (Fig. 3a) was completely different from that of the APTES-coated PC (Fig. 3d). New peaks appeared at 400 and 102 eV, corresponding to the N1s and Si2p, providing evidence of the presence of APTES on the PC surface. In the case of pristine PDMS and ECTMS-coated PDMS, no difference in the survey spectra was observed, as all atoms were the same in both substrates (Fig. S4 and S5 in the ESI†). However, the atomic concentrations changed when ECTMS was introduced on the
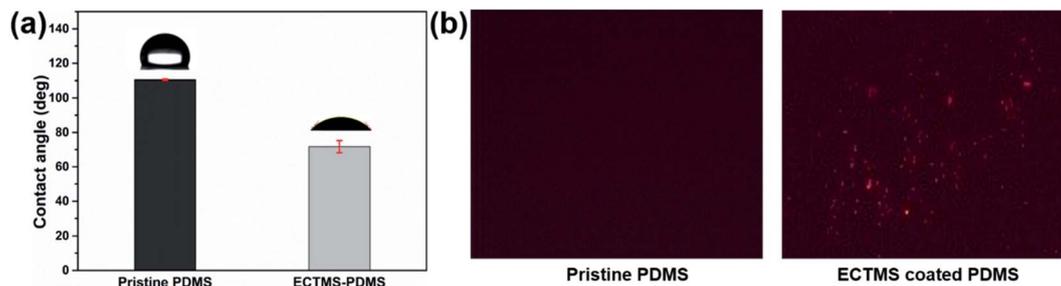
**Fig. 2** Results showing (a) contact angle measurements and (b) fluorescence measurements for pristine PDMS and ECTMS-coated PDMS.

surface of the PDMS (Table 1). As can be seen in Table 1, the concentration of O1s for ECTMS-coated PDMS (48.5%) was higher than that of the pristine PDMS (42.9%), confirming the presence of the epoxy group of ECTMS on the PDMS surface. Moreover, the variation in the other atomic concentrations such as C1s, and Si2p after the silane treatment clearly indicated the successful chemical coating of the PDMS surface. This experimental evidence confirmed that the silane reagents, such as ECTMS and APTES, were successfully coated on the surface of the PDMS and PC.

**AFM analysis.** AFM was used to examine the topographical changes in the untreated and treated surfaces. The AFM images of pristine PDMS and ECTMS-coated PDMS surfaces are shown in Fig. 4. The height of the pristine PDMS was 36.5 nm (Fig. 4a and b), and it had a smooth surface as shown by the 3D image (Fig. 4c). When ECTMS was introduced on the PDMS, the height of the surface drastically increased to 154 nm (Fig. 4d and e), and the 3D image showed that the ECTMS had strongly aggregated on the surface of the PDMS (Fig. 4f). The variations in

surface roughness after the coating of different components over the native surface can be measured using AFM analysis.[36] The calculated average roughness ($R_a$) of pristine PDMS was 4.2 nm, and it remarkably increased to 40.9 nm due to the oxygen atom of ECTMS attacking the PDMS surface during the silane treatment. This phenomenon strongly indicates that the ECTMS was successfully incorporated in the PDMS surface. Previous studies have demonstrated that the increase in the surface roughness enhances the adhesion properties of substrates,[37] and this principle is exactly followed in our ECTMS-coated PDMS. Therefore, the high adhesion properties of ECTMS-coated PDMS had robust bonding towards thermoplastics.

## Bonding strength measurement

**Tensile test.** Initially, the bonding strengths of thermoplastics–PDMS devices were evaluated by the manual peeling of the PDMS from the thermoplastics. The PDMS could not be peeled from the surface of the thermoplastic without breaking the
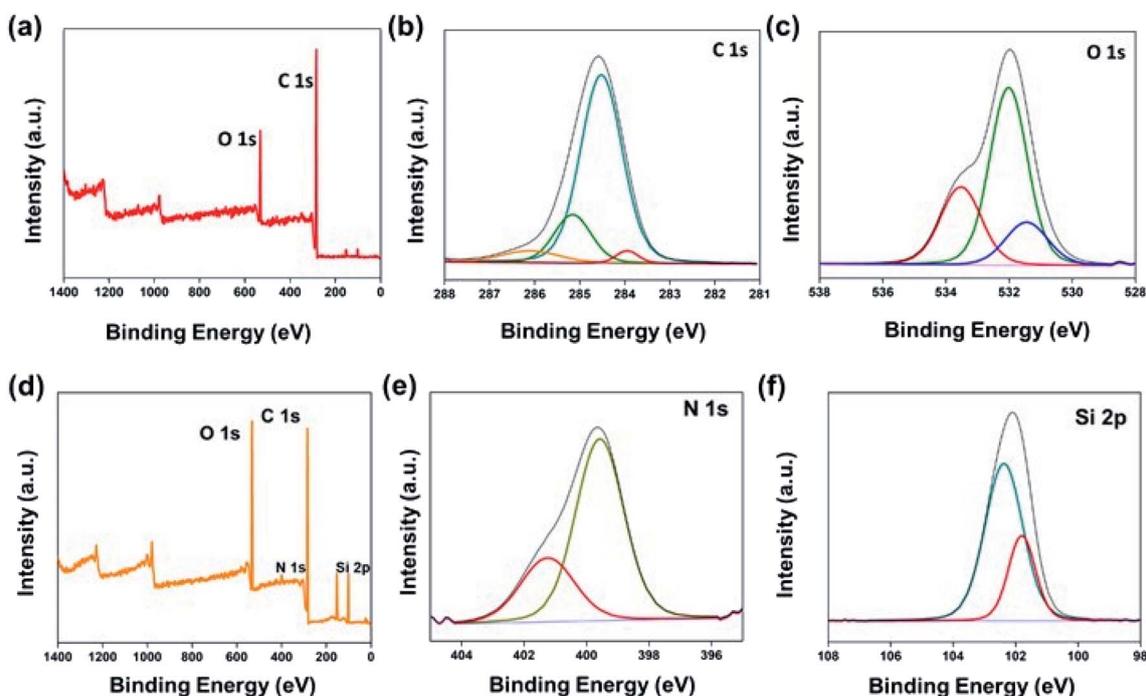


**Fig. 3** XPS for pristine PC showing (a) the survey spectrum, (b) C1s, (c) O1s, and for APTES-coated PC showing (d) the survey spectrum, (e) N1s, and (f) Si2p.

**Table 1**  Atomic ratios of pristine PDMS and ECTMS-coated PDMS

| Substrate | Spectrum | Atomic ratio (%) |
|---|---|---|
| Pristine PDMS | **O1s** | **42.9** |
| | C1s | 40.1 |
| | Si2p | 16.8 |
| ECTMS-coated PDMS | **O1s** | **48.5** |
| | C1s | 36.7 |
| | Si2p | 14.6 |

PDMS into the pieces, confirming the irreversibility of the bonding (Fig. S6 in the ESI†). The tensile strengths of the PDMS–thermoplastics devices were measured and their bond strength values were averaged as shown in Fig. 5a. The bond strengths of PDMS–thermoplastics were calculated by pulling two substrates in opposite directions. Permanent bonds were formed in all fabricated PDMS–thermoplastic assemblies, regardless of the types of thermoplastics used, which was confirmed by the ruptured PDMS attached to the thermoplastic surfaces after the detachment (Fig. 5b). The average bond strength was calculated to be approximately $274.5 \pm 27$, $591.7 \pm 44$, $594.7 \pm 25$, and $510 \pm 47$ kPa for the PDMS–PMMA, PDMS–PS, PDMS–PC, and PDMS–PET, respectively. To verify the use of chemicals for bonding, a negative control experiment was also conducted following the same experimental procedure, except for using the chemicals (APTES or ECTMS) during surface modification. However, bonding did not occur between the PDMS and thermoplastics (data not shown), promising the effectiveness of the introduced chemical bonding method. Furthermore, the bonding strengths of PDMS–PMMA ($274.5 \pm 27$ kPa) and PDMS–PC ($594.7 \pm 25$) using ECTMS were found to be significantly higher than those previously reported by our group using GPTMS as an epoxy source for bonding PDMS–PMMA (180 kPa), and PDMS–PC (178 kPa).[10] This was because the cyclohexyl epoxy group (ECTMS) is more active than the

linear chain epoxy group (GPTMS). In the bonding process, after the APTES attacks an ECTMS group, many hydroxyl (–OH) and secondary amine (–NH–) groups are formed, which improves the bonding strength further due to their intermolecular hydrogen bonding (Fig. 5c). Therefore, our chemical bonding approach is more viable and produces a greater bonding strength as compared to previously reported methods, as displayed in Table S1.†[38,39] Moreover, we have conducted experiments to check the bond strength between PDMS and PMMA using three different concentrations of ECTMS and APTES. The bond strengths were approximately 280, 285, and 305 kPa when the solution concentrations were 1%, 2%, and 5%, respectively. These results revealed that the bond strength was not dramatically increased by increasing the concentrations of the silane reagents.

**Leakage test.** The purple ink was injected at 0.1, 01, 10, 20, and 30 mL min$^{-1}$, with per-minute injection volumes corresponding to 10, 100, 1000, 2000, and 3000 times the total internal volume of the serpentine microchannel used. The microchannel did not display any leakage while using all five flow rates; a video of the experiment is attached as Movie S1 in the ESI.† The results of the leakage test confirmed that the microchannel was not clogged and distorted under this bonding method, maintaining high fidelity in the channel profile.

**Burst test.** The bond strength was further checked by infusing compressed air through the inlet into PDMS–thermoplastics microfluidic devices containing a serpentine microchannel. The burst pressure, which is defined as the maximum air pressure at which the assembled PDMS–thermoplastic microfluidic device detaches, was approximately 50, 65, 55, and 55 psi for PDMS–PMMA, PDMS–PS, PDMS–PC, and PDMS–PET, respectively. Generally, in microfluidic devices, external or internal pressures require below 50 psi when devices are in function.[40] Therefore, our chemical bonding method confirmed that the high-strength PDMS–thermoplastic hybrid devices are applicable in the microfluidic performances where high flow injection is needed.
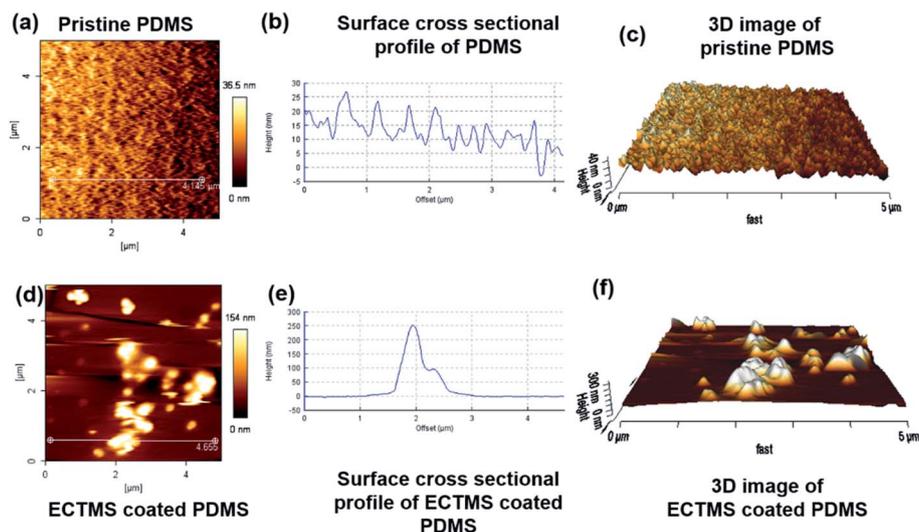


**Fig. 4**  AFM images of (a–c) pristine PDMS and (d–f) ECTMS-coated PDMS.
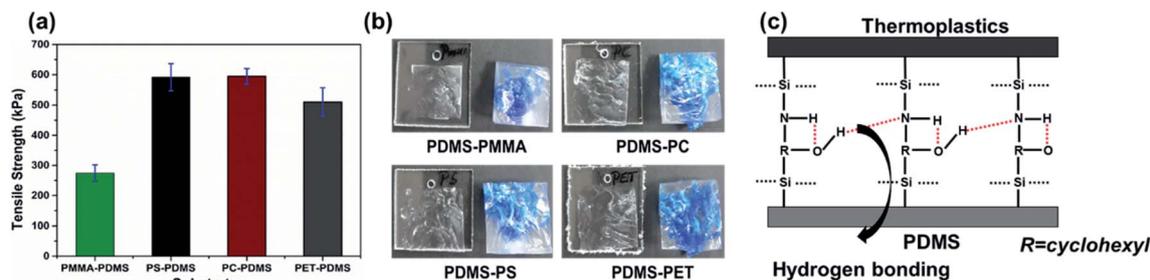
Fig. 5 Tensile strengths of PDMS–thermoplastic devices. (a) Average bonding strengths. (b) Photos showing ruptured PDMS remaining on the surface of thermoplastics. (c) Anticipated intermolecular hydrogen bonding taking place between ECTMS-coated PDMS and APTES-coated thermoplastics.

**Hydrolytic stability test.** Water is the most frequently used solvent in many LOC applications. The device bonded to channel walls is always exposed to the aqueous fluids entering through the channel. If the stability of the bond toward fluids is quite low, leakage can occur. Therefore, to perform the biological applications, the hydrolytic stability of the bonded device has to be evaluated. To verify this, the inside channel of our PDMS–PC hybrid microfluidic device was filled with water and it was completely submerged in water at 40 °C for 3 days; the same was done for another device for 12 h at 90 °C. Both devices were tested for leakage, and the results showed that no leakages were observed even at high pressure, demonstrating that the PDMS–PC microfluidic device has greater hydrolytic stability.

### CF-PCR inside the microfluidic device

Fig. 6a shows a photo of the PDMS–PC microfluidic device fabricated using the bonding method introduced in the present study. The PDMS substrate with a serpentine microchannel was successfully sealed with a flat PC substrate to perform CF-PCR. Fig. 6b shows an IR camera image of the surface temperature of the PC substrate in two temperature zones (denaturation and annealing/extension). The positioning of the microfluidic device on heaters generally follows the schematic shown in Fig. S7 in the ESI† to ensure the on-chip PCR process. According to the results, the denaturation temperature was around 94.63 ± 0.38 °C (CV 0.41% ($n = 10$)), and the annealing/extension was approximately 56.91 ± 0.21 °C (CV 0.37% ($n = 10$)) for amplifying the 210 bp of *E. coli* O157:H7. We chose PC among the various polymers since PC has a relatively high glass transition temperature (145 °C), and the surface temperature of the PC substrate was constantly maintained over 120 min (Fig. S8 in the ESI†), indicating that our microfluidic device was suitable for performing on-chip CF-PCR. The 210 bp target gene from the Shiga-toxin gene region of *E. coli* O157:H7 was successfully amplified within 30 min (Fig. 6c).

The negative (Lane 1) and positive (Lane 2) controls were performed using a thermocycler, and the results of CF-PCR are shown in Lanes 3–5 using our PDMS–PC microfluidic device. Using the hybrid PDMS–PC microfluidic device, the CF-PCR was successfully achieved to rapidly identify foodborne pathogens; the average intensity of the amplicons obtained using this method was approximately 35.53% as compared to the positive
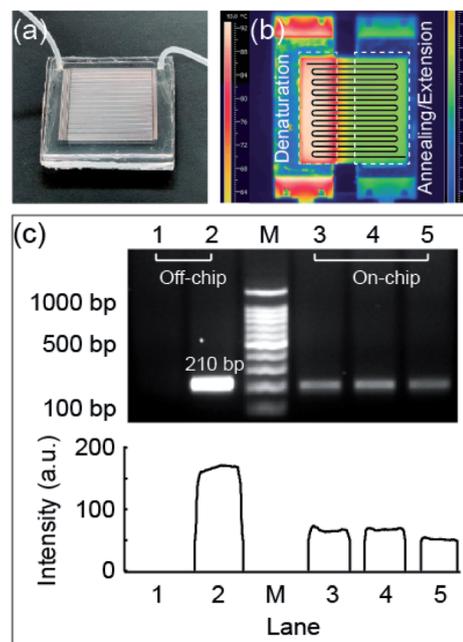


Fig. 6 (a) A photo of the hybrid PDMS–PC microfluidic device. (b) IR camera image showing the temperature profile. (c) Results of 210 bp target amplicons obtained from *E. coli* O157:H7 using a thermocycler (Lanes 1-2) and microfluidic device (Lanes 3–5). Lane M shows the 100 bp DNA size marker.

control. Also, to confirm the reproducibility of amplification using this microfluidic device, similar results were obtained after repeating the same experiment in triplicate for amplifying the 210 bp target gene. From those results, we concluded that this chemical-based bonding method for fabricating hybrid microfluidic devices has potential for CF-PCR, which always requires high temperature and pressure during the reaction.

## Conclusions

In the present study, we successfully fabricated PDMS–thermoplastic microfluidic devices at RT capable of withstanding the elevated temperatures and high pressures realized by the strong covalent carbon–nitrogen bonding using silane reagents such as cyclohexyl epoxysilane and aminosilane. Cyclohexyl

epoxysilane is highly reactive towards nucleophiles due to the ring strain of the epoxy group, which plays a crucial role in the strong PDMS–thermoplastic bond formation, the force of which was confirmed by tensile, leakage, and burst tests. Along with carbon–nitrogen bonding, the intermolecular hydrogen bond formed between hydroxyl (–OH) and secondary amine (–NH–) groups at the interface further strengthened the bonding between PDMS and thermoplastics. Moreover, the fabricated microfluidic devices can be used in cases when high-flow injection is mandatory, such as in micro-reactors and liquid chromatographic applications. According to our results, leakage did not occur even under high pressure, which was verified by the leakage test. The PDMS–PC microfluidic device was successfully adopted for performing CF-PCR owing to its excellent hydrolytic stability and has been applied to the amplification of the 210 bp gene fragment from the Shiga-toxin gene region of *E. coli* O157:H7. The introduced chemical-based bonding method is highly promising for fabricating PDMS–thermoplastic hybrid microfluidic devices for next-generation biomedical devices. It can also be anticipated that the proposed method can be used in various fields, including clinical applications, catalysis, and the food industry.

## Conflicts of interest

There are no conflicts to declare.

## Acknowledgements

## References

1 C. Zhang and D. Xing, *Chem. Rev.*, 2010, **110**, 4910–4947.
2 Y. Zheng, K. Kang, F. Xie, H. Li and M. Gao, *BioChip J*, 2019, **13**, 217–225.
3 S. Wang, S. Yu, M. S. Siedler, P. M. Ihnat, D. I. Filoti, M. Lu and L. Zuo, *Rev. Sci. Instrum.*, 2016, **87**, 105005.
4 A. Baraket, M. Lee, N. Zine, N. Yaakoubi, J. Bausells and A. Errachid, *Microchim. Acta*, 2016, **183**, 2155–2162.
5 M. K. Yuzon, J. H. Kim and S. Kim, *BioChip J*, 2019, **13**, 277–287.
6 S. G. Im, K. W. Bong, C.-H. Lee, P. S. Doyle and K. K. Gleason, *Lab Chip*, 2009, **9**, 411–416.
7 J. Xu and K. K. Gleason, *Chem. Mater.*, 2010, **22**, 1732–1738.
8 P. Gu, K. Liu, H. Chen, T. Nishida and Z. H. Fan, *Anal. Chem.*, 2011, **83**, 446–452.
9 K. Aran, L. A. Sasso, N. Kamdar and J. D. Zahn, *Lab Chip*, 2010, **10**, 548–552.
10 L. Tang and N. Y. Lee, *Lab Chip*, 2010, **10**, 1274–1280.
11 B. M. Maoz, A. Herland, O. Y. F. Henry, W. D. Leineweber, M. Yadid, J. Doyle, R. Mannix, V. J. Kujala, E. A. FitzGerald, K. K. Parker and D. E. Ingber, *Lab Chip*, 2017, **17**, 2294–2302.
12 O. Y. F. Henry, R. Villenave, M. J. Cronce, W. D. Leineweber, M. A. Benz and D. E. Ingber, *Lab Chip*, 2017, **17**, 2264–2271.
13 B. Cortese, M. C. Mowlem and H. Morgan, *Sens. Actuators, B*, 2011, **160**, 1473–1480.
14 I. R. G. Ogilvie, V. J. Sieben, B. Cortese, M. C. Mowlem and H. Morgan, *Lab Chip*, 2011, **11**, 2455–2459.
15 W. Wu, J. Wu, J.-H. Kim and N. Y. Lee, *Lab Chip*, 2015, **15**, 2819–2825.
16 K. S. Lee and R. J. Ram, *Lab Chip*, 2009, **9**, 1618–1624.
17 M. Tweedie, D. Sun, B. Ward and P. D. Maguire, *Lab Chip*, 2019, **19**, 1287–1295.
18 T. Nguyen, S. H. Jung, M. S. Lee, T.-E. Park, S.-k. Ahn and J. H. Kang, *Lab Chip*, 2019, **19**, 3706–3713.
19 L. Gorgannezhad, H. Stratton and N.-T. Nguyen, *Micromachines*, 2019, **10**, 408.
20 Y. Ding, J. Choo and A. J. deMello, *Microfluid. Nanofluid.*, 2017, **21**, 58.
21 H. Yang, Z. Chen, X. Cao, Z. Li, S. Stavrakis, J. Choo, A. J. deMello, P. D. Howes and N. He, *Anal. Bioanal. Chem.*, 2018, **410**, 7019–7030.
22 O. Frey, S. Bonneick, A. Hierlemann and J. Lichtenberg, *Biomed. Microdevices*, 2007, **9**, 711–718.
23 K. T. L. Trinh, H. Zhang, D.-J. Kang, S.-H. Kahng, B. D. Tall and N. Y. Lee, *Int Neurourol J*, 2016, **20**, S38–S48.
24 K. T. L. Trinh and N. Y. Lee, *Talanta*, 2018, **176**, 544–550.
25 W. Wu, K. T. L. Trinh and N. Y. Lee, *Analyst*, 2015, **140**, 1416–1420.
26 A. C. Hatch, T. Ray, K. Lintecum and C. Youngbull, *Lab Chip*, 2014, **14**, 562–568.
27 D. Rodriguez-Lazaro, P. Gonzalez-García, E. Delibato, D. De Medici, R. M. García-Gimeno, A. Valero and M. Hernandez, *Int. J. Food Microbiol.*, 2014, **184**, 113–120.
28 A. Abd-Elmagid, P. A. Garrido, R. Hunger, J. L. Lyles, M. A. Mansfield, B. K. Gugino, D. L. Smith, H. A. Melouk and C. D. Garzon, *J. Microbiol. Methods*, 2013, **92**, 293–300.
29 L. Cao, X. Cui, J. Hu, Z. Li, J. R. Choi, Q. Yang, M. Lin, L. Ying Hui and F. Xu, *Biosens. Bioelectron.*, 2017, **90**, 459–474.
30 J. Jeon, N. Choi, H. Chen, J. I. Moon, L. Chen and J. Choo, *Lab Chip*, 2019, **19**, 674–681.
31 Y. Zhang, K. T. L. Trinh, I.-S. Yoo and N. Y. Lee, *Sens. Actuators, B*, 2014, **202**, 1281–1289.
32 W. Wu, K. T. L. Trinh, Y. Zhang and N. Y. Lee, *RSC Adv.*, 2015, **5**, 12071–12077.
33 T. T. Nguyen, K. T. L. Trinh, W. J. Yoon, N. Y. Lee and H. Ju, *Sens. Actuators, B*, 2017, **242**, 1–8.
34 K. T. L. Trinh, Q. N. Pham and N. Y. Lee, *Sens. Actuators, B*, 2019, **282**, 1008–1017.
35 T. Trantidou, Y. Elani, E. Parsons and O. Ces, *Microsyst. Nanoeng.*, 2017, **3**, 16091.
36 V. Sunkara, D.-K. Park and Y.-K. Cho, *RSC Adv.*, 2012, **2**, 9066–9070.
37 D. E. Packham, *J. Adhes.*, 1992, **39**, 137–144.
38 H. Zhang and N. Y. Lee, *Appl. Surf. Sci.*, 2015, **327**, 233–240.
39 V. Sunkara, D.-K. Park, H. Hwang, R. Chantiwas, S. A. Soper and Y.-K. Cho, *Lab Chip*, 2011, **11**, 962–965.
40 X. Wang, D. T. T. Phan, D. Zhao, S. C. George, C. C. W. Hughes and A. P. Lee, *Lab Chip*, 2016, **16**, 868–876.